J. of Cardiovasc. Trans. Res. (2010) 3:135–146
DOI 10.1007/s12265-009-9138-1

Intramyocardial Navigation and Mapping for Stem Cell Delivery

Peter J. Psaltis · Andrew C. W. Zannettino · Stan Gronthos · Stephen G. Worthley

Received: 5 September 2009 / Accepted: 28 September 2009 / Published online: 23 October 2009

Abstract Method for delivery remains a central component of stem cell-based cardiovascular research. Comparative studies have demonstrated the advantages of administering cell therapy directly into the myocardium, as distinct from infusing cells into the systemic or coronary vasculature. Intramyocardial delivery can be achieved either transepicardially or transendocardially. The latter involves percutaneous, femoral arterial access and the retrograde passage of specially designed injection catheters into the left ventricle, making it less invasive and more relevant to wider clinical practice. Imaging-based navigation plays an important role in guiding catheter manipulation and directing endomyocardial injections. The most established strategy for three-dimensional, intracardiac navigation is currently endoventricular, electromechanical mapping, which offers superior spatial orientation compared to simple x-ray fluoroscopy. Its provision of point-by-point, electrophysiologic and motion data also allows characterization of regional myocardial viability, perfusion, and function, especially in the setting of ischemic heart disease. Integrating the mapping catheter with an injection port enables this diagnostic information to facilitate the targeting of intramyocardial stem cell delivery. This review discusses the diagnostic accuracy and expanding therapeutic application of electromechanical navigation in cell-based research and describes exciting developments which will improve the technology's sensing capabilities, image registration, and delivery precision in the near future.

Keywords Cardiac Navigation · Electromechanical Mapping · Intramyocardial Delivery · Myocardial Viability · NOGA · Stem Cell Therapy

P. J. Psaltis (✉) · S. G. Worthley
Cardiovascular Research Centre, Department of Cardiology, Royal Adelaide Hospital and the Department of Medicine, University of Adelaide,
Adelaide, South Australia 5000, Australia
e-mail: peter.psaltis@adelaide.edu.au

P. J. Psaltis · A. C. W. Zannettino · S. Gronthos
Bone and Cancer Laboratories, Division of Haematology, Institute of Medical and Veterinary Science/Hanson Institute & Centre for Stem Cell Research, Robinson Institute, University of Adelaide,
Adelaide, Australia

Introduction

Despite the advances in therapy, cardiovascular disease remains the leading cause of morbidity and mortality in Western communities and represents a growing economic burden to most health systems. This has led to the emergence of novel therapeutic approaches for the treatment of ischemic heart disease (IHD) and cardiomyopathy, including gene transfer, growth factor/cytokine administration, and cell transplantation. Cellular therapy has evolved quickly over the last 10 years, both at the level of in vitro and in vivo preclinical research and more recently in clinical trials of myocardial infarction (MI), IHD, and congestive cardiac failure [45]. However, there remain many challenges that need to be addressed if cell transplantation is to become widely used in clinical practice in the future.

In addition to the type of cell therapy, another key issue is the method of cell delivery. Although there are several options available for administering cells to the heart, recent studies have highlighted the advantages of direct injection into the myocardium, as compared to systemic or intracoronary, vascular infusion [33, 52]. In this review, we focus on the clinically relevant strategy of percutaneous, transendocardial injection, facilitated by intramyocardial

navigation. The current mainstay of this approach is the endoventricular electromechanical mapping system, NOGA® XP (NOGA® XP Cardiac Navigation system, Biologics Delivery Systems Group, Cordis Corporation, Diamond Bar, CA, USA), which is integrated with a multicomponent injection catheter (MyoStar™, Biosense-Webster, Diamond Bar, CA, USA). The unique features of this sophisticated technology will be discussed, with particular reference to its diagnostic capability and therapeutic utility in the navigated delivery of cell therapy.

Methods for Cell Delivery

The main objectives of cell delivery are to ensure safe transplantation, maximum retention of cells within the target myocardium, and adequate local engraftment and function at this site. Cells can be directed to the heart (1) systemically (e.g., peripheral venous injection, growth factor mobilization), (2) by regional coronary vascular infusion, or (3) by local, direct myocardial injection [59]. The choice of delivery route is dependent on both the disease process requiring treatment and the type of cell to be transplanted. To date, myocardial retention of cells has been disappointing with both vascular and direct routes of administration [33], and it remains difficult to establish which delivery system will fulfill most of the intended need.

Although the practicality of transcoronary infusion has led to its consistent use in clinical studies of acute MI [64], IHD [15], and nonischemic cardiomyopathy (NICM) [18], preclinical evidence suggests that this approach may be limited by non-cardiac entrapment of cells and aggregation of some cell types in the coronary microvasculature [19, 76]. Unlike intracoronary infusion, direct intramyocardial injection targets specific regions of myocardium without relying on the upregulation of inflammatory signals to assist transvascular cell migration and tissue invasion. Comparative evidence indicates that this approach achieves better myocardial cell retention than intravascular infusion, possibly resulting in greater therapeutic effects [33, 52].

Intramyocardial injection can be achieved transepicardially or transendocardially. Although these two approaches are probably similar in their ability to disperse cells throughout the myocardial wall, comparative assessment has been limited [24]. Transepicardial delivery has been most commonly undertaken following sternotomy for concurrent coronary artery bypass grafting [48], although mini-thoracotomy or subdiaphragmatic access [56] and catheter-based injection from inside the coronary venous system [65] have also been described. The less invasive strategy of transendocardial delivery is performed via a percutaneous, femoral arterial approach using a catheter that is passed retrogradely across the aortic valve into the left ventricle (LV). Advantages of this method are that it can be used on high-risk patients without the need for general anesthesia or sternotomy, and may be safely repeated for serial treatments [23, 55].

Transendocardial Delivery Systems

A variety of catheter systems are available for transendocardial injection, sharing a multicomponent catheter design that consists of a core needle for cell delivery and a support catheter for directing the needle to the target sites for injection. These include the Stilleto™ (Boston Scientific, Natick, MA, USA) [30], BioCardia™ (BioCardia, South San Francisco, CA, USA) [1], MyoCath™ (Bioheart Inc., Sunrise, FL, USA) [35] and MyoStar™ [12] catheters.

Typically, the Stilleto™, BioCardia™, and MyoCath™ catheter systems are not integrated with additional navigational or targeting capability, beyond two-dimensional (2D) x-ray fluoroscopy. Even with biplane imaging, conventional x-ray guidance is limited by its lack of 3D precision for catheter orientation and its failure to characterize the status of the underlying myocardium; this may potentially compromise the safety and efficacy of cell delivery, if cells are inadvertently injected into healthy tissue. These concerns may be partly overcome by performing adjunctive imaging (e.g., single photon emission computed tomography (SPECT) or magnetic resonance imaging (MRI)) prior to fluoroscopic guidance, to help pre-select the myocardial segments requiring injection [11]. An alternative strategy that remains investigational has been to modify the aforementioned catheters to allow coupling with real-time navigation by customized MRI (e.g., Stiletto [13], MyoCath [9]) or 3D echocardiography [8].

Electromechanical Navigation

The unique feature of the MyoStar™ injection catheter is that it is integrated with the NOGA® system of non-fluoroscopic, magnetic, electromechanical guidance [61]. This navigation technology was developed over a decade ago as an extension of the CARTO™ electroanatomical mapping system [5] and in recent years has been updated to a Windows XP platform, giving rise to its current incarnation: NOGA® XP. NOGA® incorporates spatial, electrophysiological, and mechanical information in real-time to reconstruct the heart's endocardial surface in 3D. The technology has been predominantly used for mapping the LV, particularly in experimental and clinical studies of IHD. In this context, local electrical and mechanical measurements have been combined to evaluate regional myocardial function, viability, and ischemia, in turn enabling targeted delivery of intramyocardial therapies, including laser energy [44], gene [73], and cell [51] transplantation.

NOGA® System Components

The current NOGA® XP system comprises the following key elements:

- A location pad positioned underneath the subject, consisting of three coils that generate ultralow magnetic fields (5×10^{-5} to 5×10^{-6} Tesla).
- A fixed-position reference catheter (REFSTAR™ with QWIKPATCH® External Reference Patch, Biosense-Webster) which is attached to the subject's back and has a miniature magnetic field sensor to improve location accuracy during mapping.
- A 7-Fr steerable mapping catheter (NogaStar®, Biologics Delivery Systems Group). Miniature, passive, magnetic sensors proximal to the catheter tip detect and record the emitted magnetic signals from the location pad to provide accurate resolution of the location (x, y, and z) and orientation (roll, pitch, and yaw) of the catheter tip in six degrees of freedom. The catheter also contains distal unipolar and bipolar electrodes that measure voltage potentials from the endomyocardium.
- A computer and Silicon Graphics workstation (Mountain View, CA, USA) that processes data. The workstation monitor, which can be modified to suit the operator's preferences, shows updated electrogram signals from both body surface and catheter, displays information about electrogram and catheter stability, and constantly updates the reconstructed, color-coded maps of the LV.

For therapeutic applications, these components are complemented by the 8-Fr MyoStar™ delivery catheter. This consists of a support catheter with sensing properties and an injection component which is fitted with a retractable, straight, 27 gauge, nitinol needle.

Electromechanical Mapping Procedure

The electromechanical mapping procedure has been described in detail elsewhere [61]. Fluoroscopic guidance is required initially to advance the NogaStar® catheter retrogradely into the LV cavity and sample the first few endocardial points to initiate the NOGA® map. Thereafter, there is minimal reliance on fluoroscopy as the navigation system can locate the catheter in real-time within the boundaries of the reconstructed cardiac chamber. Endocardial points are sampled quickly and sequentially from each region of the LV, using well-established criteria for endocardial-catheter tip contact and stability, as well as point density [61]. An adjustable "fill threshold" (usually set to 15 mm) allows the system to fill-in the surface between sampled points. With the current Windows XP platform, mapping can be completed comfortably inside of 45 min, and despite its invasive nature, the procedure is usually well tolerated, with few published reports of complications (e.g., sustained arrhythmia, embolization of LV thrombus, and hemorrhagic pericardial effusion).

Electromechanical Parameters

As the LV is being reconstructed, NOGA® determines its center of mass and can derive its end-diastolic and end-systolic volumes, along with stroke volume and ejection fraction (EF) [26].

The sensing catheters acquire electrical data at each endocardial site in the form of local activation time (ms), unipolar voltage (UV), and bipolar voltage (BV) amplitudes (mV). Mechanical information is presented as a parameter called linear local shortening (LLS), which is algorithmically calculated as the average change in distance between the index catheter point and its surrounding points from end-diastole to end-systole, with preferential weighting given to points within an 8–15-mm distance. This is to accommodate the non-uniform density of point sampling and to minimize the confounding influence of point clustering or myocardial tethering of regions adjacent to actively contracting myocardium. Local shortening results are presented as percentages, which become smaller or even negative if regional contractility is reduced or paradoxical.

The map reconstruction for each of these parameters is accessible in real-time, in a variety of projections, including a nine-segment (or 13-segment) Bull's-eye view which displays the regional distribution of data. For voltage and local shortening maps, the color-scheme usually depicts regions with high (normal) values as blue-purple and those with reduced values as yellow-red (Figs. 1 and 3). The thresholds for the color scale can be manually adjusted to the optimal discriminatory values that apply to the underlying cardiac disease process or the species being studied. The system also provides the average measurements for each segment obtained from all of its sampled points, thus facilitating quantitative, inter-segmental comparisons.

Diagnostic Accuracy of Electromechanical Mapping

Early evaluation of NOGA® confirmed the stability of the mapping catheter during the cardiac cycle and verified the system's accuracy and reproducibility for locating catheter tip position (to less than 1 mm), measuring distances, recording unipolar intracardiac signals and creating activation time maps [25, 66].

Ischemic Heart Disease

The utility of electromechanical navigation is underpinned by the electromechanical coupling of cardiomyocytes. The

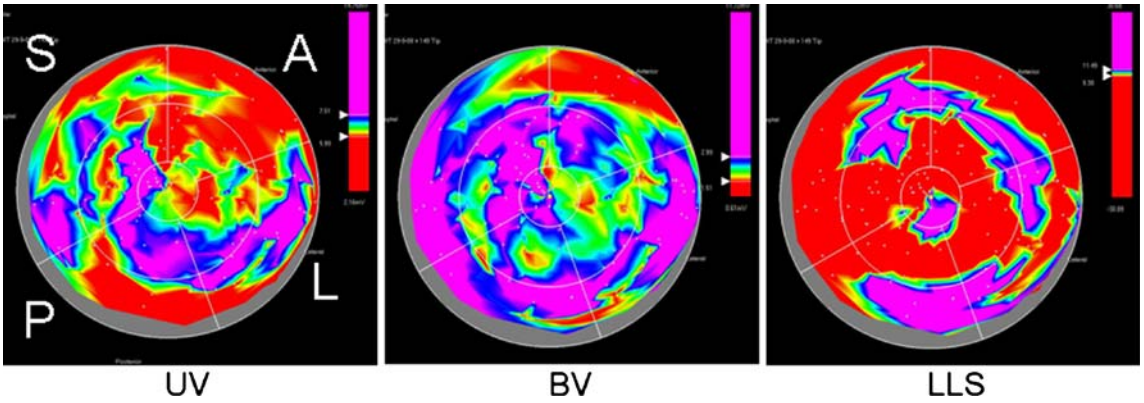

Fig. 1 Electromechanical mapping in nonischemic cardiomyopathy. Representative, nine-segment, Bull's-eye projections from a sheep with anthracycline-induced nonischemic cardiomyopathy (ejection fraction 30.5%). Unipolar voltage (UV), bipolar voltage (BV), and linear local shortening (LLS) maps demonstrate the heterogeneous reduction of these parameters in this preclinical model. Color-scales have been set to reflect optimal discriminatory thresholds for identifying myocardial fibrosis (UV: *Red* ≤6 mV, *Purple* ≥7.5 mV; BV: *Red* ≤1.5 mV, *Purple* ≥3.0 mV; LLS: *Red* ≤9.3%, *Purple* ≥11.5%). In this context, we have found that LLS displays the best accuracy for detecting segments with foci of replacement fibrosis, followed by UV amplitude. *A*, anterior; *L*, lateral; *P*, posterior; *S*, septal

accuracy of endocardial voltage amplitudes and local shortening ratios for identifying reductions in myocardial viability, perfusion, and function has been investigated in studies of MI [39, 54], reversible ischemia [39], and ischemic cardiomyopathy [6]. NOGA®-derived measurements have been cross-referenced against histological measurement of scar tissue [78] and against other myocardial imaging techniques, such as radionuclide scintigraphy (SPECT, 18-fluoro-2-deoxy-D-glucose positron emission tomography) [29, 77], rest and stress transthoracic echocardiography [38, 57], and MRI [54].

Typically, normal human LV myocardium exhibits BV amplitudes greater than 1.5–2 mV [34] and UV amplitudes greater than 10–12 mV [37, 39]. Reduced endocardial voltage indicates electrically abnormal tissue, most commonly due to infarct scar or ischemic hibernation [20, 39, 54]. In the context of IHD, the integration of complementary mechanical data assists in distinguishing non-viable scar from viable, peri-infarct tissue or dysfunctional, hibernating myocardium. The cut-off threshold level for normal LLS ratios has varied between clinical studies, from 9% [37] to 12% [40]. Regions of akinetic/dyskinetic scar are easily delineated by their very low shortening ratio (LLS <2–3%) [39], while results are intermediate for myocardium with reversible ischemia, depending on its severity and the presence of hibernation [21, 37].

Electromechanical profiles in IHD have been characterized by (1) coupling of electrical and mechanical impairment for irreversible MI and scar [39], (2) preservation of electrical activity with reduced endocardial shortening for stunned or hibernating myocardium [21], or (3) preservation of both electrical and mechanical function for ischemic myocardium in which perfusion is normal at rest. There is conflicting evidence as to which parameter is most accurate for

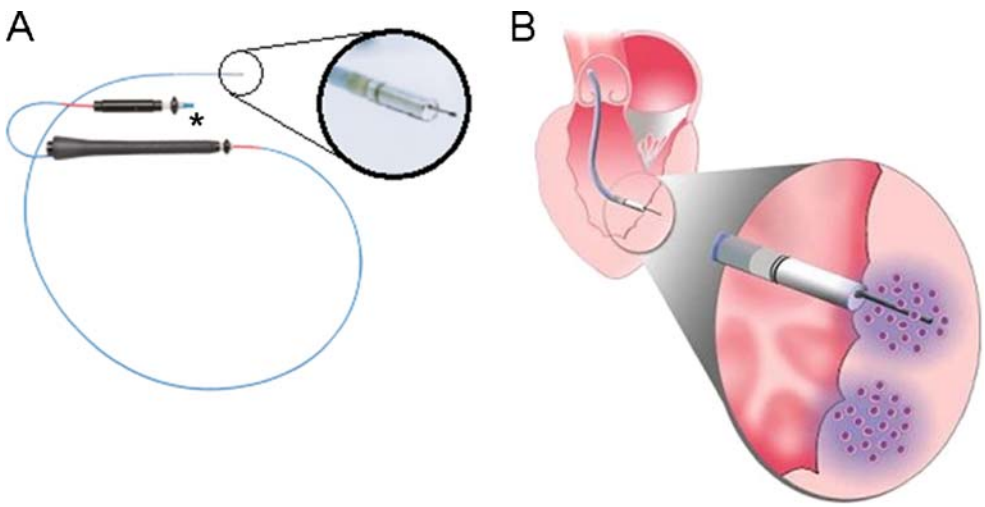

Fig. 2 Transendocardial injection with MyoStar™ catheter. The MyoStar™ injection catheter with inset view of catheter tip and nitinol needle (**a**). The adjustable injector thumb knob and Luer lock fitting for connection to the injection syringe can be seen at the catheter's proximal end (*asterisk*). Adjacent is a schematic showing the catheter's retrograde, transendocardial approach into the left ventricle, with the injection needle extruded into the endomyocardium (**b**). Images courtesy of the Biologics Delivery Systems Group Inc.

individually characterizing myocardial viability [57, 78]. Endocardial voltage amplitudes appear to correlate better with myocardial viability than perfusion [29]. Generally, optimal threshold values for defining viable tissue have been reported in the range of 6.4–7.5 mV for UV, with moderately good sensitivity and specificity of approximately 80% [20, 37, 40, 54].

Nonischemic Heart Disease

In contrast to IHD, there are currently no published reports evaluating electromechanical characterization in nonischemic cardiac disease. We have recently investigated the accuracy of NOGA® XP for detecting segmental myocardial fibrosis in NICM, using an ovine model of anthracycline-induced cardiac dysfunction (Fig. 1) [58]. Histological validation demonstrated that threshold values <11.5% for LLS and <7.5 mV for UV identified myocardium with >10% fibrosis burden (usually comprising midmural or subepicardial foci of replacement fibrosis), with sensitivity and specificity of 75–85% (Psaltis et al. 2009a in submission). Notably, LLS also showed potential to distinguish regions of intermediate, reactive fibrosis from normal myocardium, while BV amplitude was the least accurate parameter. In nonischemic disease, the reliability of endocardial electrogram signals may be hindered by the non-subendocardial location of myocardial fibrosis.

Limitations to Accuracy

A major limitation to the diagnostic performance of NOGA® arises from the considerable overlap of electrical and mechanical data between normal and abnormal myocardium [6, 37]. This leads to difficulty in establishing consistent electrical or mechanical threshold values, especially for distinguishing between intermediate grades of myocardial viability, function, or perfusion [37, 54]. It has been suggested that accuracy may be enhanced by normalizing segmental results within an individual heart to the segment which has the most preserved measurements of voltage or mechanical shortening [6].

Electromechanical navigation can also be compromised by artifact due to positional shift of the heart during the mapping procedure, either from respiratory motion, subject movement, or catheter-induced bundle branch block. As NOGA® does not provide visual verification of interventricular septal position, variations of cardiac orientation within the thorax may not be identified and may result in misrepresentation of LV segments. Voltage mapping may be confounded by far-field noise for UV signals and catheter tip orientation for BV. Indeed, the utility of bipolar signals remains contentious, despite its widespread use for arrhythmic substrate mapping [34], and this parameter has been largely overlooked in recent descriptions of electromechanical navigation.

Navigated Transendocardial Injection

Although NOGA®'s clinical application has not been consolidated as a diagnostic or prognostic adjunct for the routine assessment of IHD, the technology's special properties have ensured its relevance as a navigation system for guiding intra-myocardial interventions, including the transplantation of stem cells (Fig. 2).

Despite the high cost of the NOGA®/MyoStar™ system, it has the important advantage compared to simple fluoroscopic guidance of providing 3D visualization of the density and distribution of injection sites. Electromechanical mapping is also unique in its ability to provide real-time characterization of watershed areas of myocardial perfusion and viability. This allows it to delineate stunned myocardium surrounding MI, hibernating tissue in chronic IHD and foci of replacement fibrosis in NICM, all of which are pathological targets for cell-based intervention.

Injection Procedure

Prior to the NOGA®/MyoStar™ injection procedure, the catheter is primed with the injectate solution. The extended needle length is then checked and adjusted (usually to 4–6 mm) by a proximal handle mechanism that consists of an adjustable injector thumb knob and a Luer hub for connection of the injection syringe. Injections are performed by two operators, one of whom positions the catheter at the targeted endomyocardium, while the other delivers the injection, at a rate of approximately 0.l mL over 15 s. During injections, the NOGA® workstation provides feedback about the stability of catheter and needle position, and electromechanical maps should be repeatedly updated with a new mark for each injection site. Procedural time varies depending on the number of injections, but is usually in the order of 30–45 min.

Accuracy and Safety of Injections

The feasibility and safety of NOGA®-guided myocardial injection was initially demonstrated by injecting methylene blue dye and gene vectors in preclinical studies [41, 74]. Procedural complications (e.g., sustained arrhythmia, cardiac perforation, and elevated cardiac biomarkers) were not observed. In one study, histological analysis detected the presence of more than 90% of attempted injection tracks after 24 h [41]. Needle extensions of 3–4 mm resulted in myocardial staining to an average depth of approximately 7 mm (range 2–11 mm) and width of 2.3 mm (range of 1–9 mm), and efficiency was found to be similar to that

achieved by the transepicardial route. Less than 3% of injection sites demonstrated epicardial staining, and most of these were associated with delivery into the LV apex.

Effective deposition has also been reported after transendocardial injection of albumin (simulating growth factors) and colloid albumin (simulating adenovirus or microspheres) [68], skeletal muscle precursor cells [7], and feridex-labeled mononuclear leukocytes [43]. However, retention may be compromised by rapid wash-out from the myocardium due to a combination of channel leakage, venous, and lymphatic return [30, 63, 68].

Application in Studies of Cell Therapy

The NOGA®/MyoStar™ platform has been widely applied both preclinically and clinically for the transendocardial injection of cells to ischemic myocardium (Table 1). Various cell types have been injected including skeletal myoblasts (SkM) [12, 67, 69], unfractionated bone marrow (BM) cells [2, 22, 42, 51, 72], $CD34^+$ progenitor cells [46], and mesenchymal stromal/stem cells (MSC) [52]. Serial electromechanical mapping has also been used during follow-up to assess for improvement in myocardial viability after cell therapy [12, 42], although its accuracy for this purpose probably warrants further validation.

There has been reassuring evidence from studies with SkM [7, 49] and MSC [32] that cells are biocompatible with the injection needle and that the injection process does not substantially compromise cell viability, biology, or function. Clinical studies have reported few instances of procedural complications [2, 3, 42]. However, special caution should be employed if injecting into the basal septum (risk of conduction block and arrhythmia), LV apex, or into dense scar tissue (risk of perforation).

Acute Myocardial Infarction

By distinguishing between non-viable infarct and stunned/hibernating myocardium, electromechanical guidance can target cell injections to peri-infarct regions to attenuate post-MI LV remodeling. With current adult cell-therapies, most of this benefit is probably mediated by indirect protection of vulnerable cardiomyocytes (e.g., through paracrine support and neovascularization) as distinct from true regeneration of "lost" cardiac cell mass [28, 62].

The safety of transendocardial injection in the early post-MI period has been demonstrated by preclinical research using BM MSC [1], although new evidence has indicated that safety and efficacy may be superior when cells are administered on day 10 post-MI, rather than day 5 [16]. In a recent "first-in-man" study, autologous BM mononuclear cells (MNC) were safely delivered to patients with LV EF <40%, 10.5±5 days after presenting MI [42]. Twenty injection sites were delivered into the ischemic area at risk, as defined by a normalized UV threshold of <68%, although non-viable myocardium (nominal UV amplitude <5 mV) was excluded from treatment. Cell transplantation did not appear to cause systemic or local inflammation, exacerbate ischemic insult, or induce arrhythmia in either the short or long-term (12 months). In the absence of a control group, conclusions about the effectiveness of treatment were limited, but LV EF showed an absolute increase of approximately 6%.

The MYSTAR study has recently finished enrolment as the first randomized trial to compare the effects of intracoronary and combined (transendocardial and intracoronary) delivery of BM cells, in both the early (3–6 weeks) and late (3–4 months) periods after MI. Preliminary results have been reported, showing that combined delivery at either time-point achieves moderate benefit to LV function and infarct size [31].

Refractory Angina

The pro-angiogenic potential of BM-derived cells has led to their evaluation in chronic, symptomatic IHD [2, 22, 72]. The goal of therapy in this scenario is to achieve improvement in myocardial perfusion and angina symptoms. Compared to acute MI, chronic IHD is probably associated with less local and systemic homing signals to mobilize cells to the myocardium from the circulation. Consequently, transendocardial injection has been a popular choice for delivery in this context (Fig. 3) and is more applicable than intracoronary infusion, especially in patients with occlusive, diffuse coronary disease, not amenable to revascularization.

Several groups have demonstrated benefit to symptom class and exercise capacity following NOGA®-guided delivery of unfractionated BM cells [2, 22, 72, 75] or mobilized $CD34^+$ cells [46], in patients with refractory angina pectoris. In a recent randomized study, BM MNC therapy also resulted in greater reductions in the summed myocardial stress-perfusion score and the number of ischemic myocardial segments, than were observed after placebo intervention [75].

Cardiomyopathy

In cases where ischemic myocardial hibernation has resulted in cardiomyopathy, cell-derived neovascularization may provide benefit to regional and global contractility. In an early, non-randomized study of patients with IHD and marked reduction of LV EF (mean 20%), NOGA® guidance was used to transplant BM MNC into ischemic regions that had preserved UV amplitude (≥6.9 mV) and viability. Injections were well tolerated and resulted in

Table 1 Clinical trials using electromechanical navigation for cell delivery

Trial	Study design	Patient *N*	Cell type/dose	Follow-up/results
Myocardial infarction				
Krause [42]	Non-controlled; single center	20	BM MNC 2×10^8	6–12 months: ↑ EF, ↑ UV
MYSTAR[a] [31]	RCT	30 early 30 late	BM MNC 2×10^8 IM 1.3×10^9 IC	9–12 months: ↑ EF, ↓ MI size
Chronic symptomatic ischemic heart disease				
Beeres [2]	Non-controlled; single center	25	BM MNC 8.5×10^7	12 months: ↑ EF, ↓ ischemia, improved symptoms
Fuchs [22]	Non-controlled; multicenter	27	BMC 2.8×10^7 $CD45^+$/mL	3–12 months: ↓ CCS class, ↑ exercise capacity, ↓ ischemia
Losordo [46]	RDBPCT; dose-escalation; multicenter	18 Rx 6 placebo	G-CSF mobilization + $CD34^+$ cells 0.5, 1, 5×10^5/kg	3–6 months: trends toward improved symptoms
Protect-CAD [72]	RBPCT; dose-comparison; multicenter	19 Rx 9 placebo	BM MNC 1.7×10^7 (n=9) 4.2×10^7 (n=10)	6 months: ↑ EF, ↓ NYHA class, ↑ exercise capacity
van Ramshorst [75]	RDBPCT; single center	25 Rx 24 placebo	BM MNC 1.0×10^8	3 months: ↑ EF, ↓ ischemia 6 months: ↓ CCS class, ↑ exercise capacity
Ischemic cardiomyopathy				
Smits [67]	Non-controlled; single center	5	SkM 2.0×10^8	6 months: ↑ EF, ↑ regional wall motion
Perin [50, 51]	Non-randomized; controlled; single center	11 Rx 9 control	BM MNC 3.0×10^7	2–4 months: ↑ EF 6–12 months: ↑ exercise capacity, ↓ ischemia
CAuSMIC [12]	RPCT; dose-escalation; single center	12 Rx 11 placebo	SkM 3, 10, 30, 60×10^7	12 months: improved symptoms, ↑ UV

Cell doses are approximate and were obtained from the mean or median value reported in the respective studies

BM bone marrow, *BMC* bone marrow cells, *CCS* Canadian Cardiovascular Society, *EF* ejection fraction, *IC* intracoronary; *IM* intramyocardial, *MI* myocardial infarct, *MNC* mononuclear cells, *NYHA* New York Heart Association, *R(DB)PCT* randomized (double-blinded) placebo-controlled trial; *Rx* cell treatment; *SkM* skeletal myoblasts; *UV* unipolar voltage amplitude; ↑ increased; ↓ decreased

[a] MYSTAR study compared timing of delivery for combined intramyocardial and intracoronary routes

substantial improvement in reversible perfusion defects, accompanied by increases in regional and global myocardial function after 4 months [50]. Clinical angina scores and physiological parameters of myocardial performance on exercise testing also improved. Symptomatic benefits were sustained at 12 months, as was myocardial perfusion; however, the improvements in LV EF were no longer significant [51]. Arrhythmias were not observed as an adverse outcome in these patients, nor were there histological changes associated with abnormal cell growth [14].

In the context of post-MI cardiomyopathy, the main objective of cell transplantation is to replace scarred myocardium with functional, contractile heart tissue. This remains particularly challenging, as current cell therapies are limited by issues of poor engraftment and inadequate regeneration of the damaged cellular components. Skeletal muscle precursors continue to attract interest in this setting, largely because of their contractile and ischemia-resistant properties. Various studies have injected these cells into patients with post-MI cardiomyopathy, either transepicardially [48] or by electromechanical guidance [12, 69]. Twelve-month data from the CAuSMIC study has recently shown benefits in symptom class and UV amplitude in treated patients compared to controls, with non-significant reduction in LV dimensions [12]. This has paved the way for the CAuSMIC II study which is ongoing.

By comparison to ischemic cardiomyopathy, there has been a paucity of cell-based research in NICM, both at preclinical and clinical levels. Nonischemic disease provides unique challenges to cell biology and delivery, due to differences in myocardial homing mechanisms [71] and the variable nature of its etiology and pathology [10]. We have

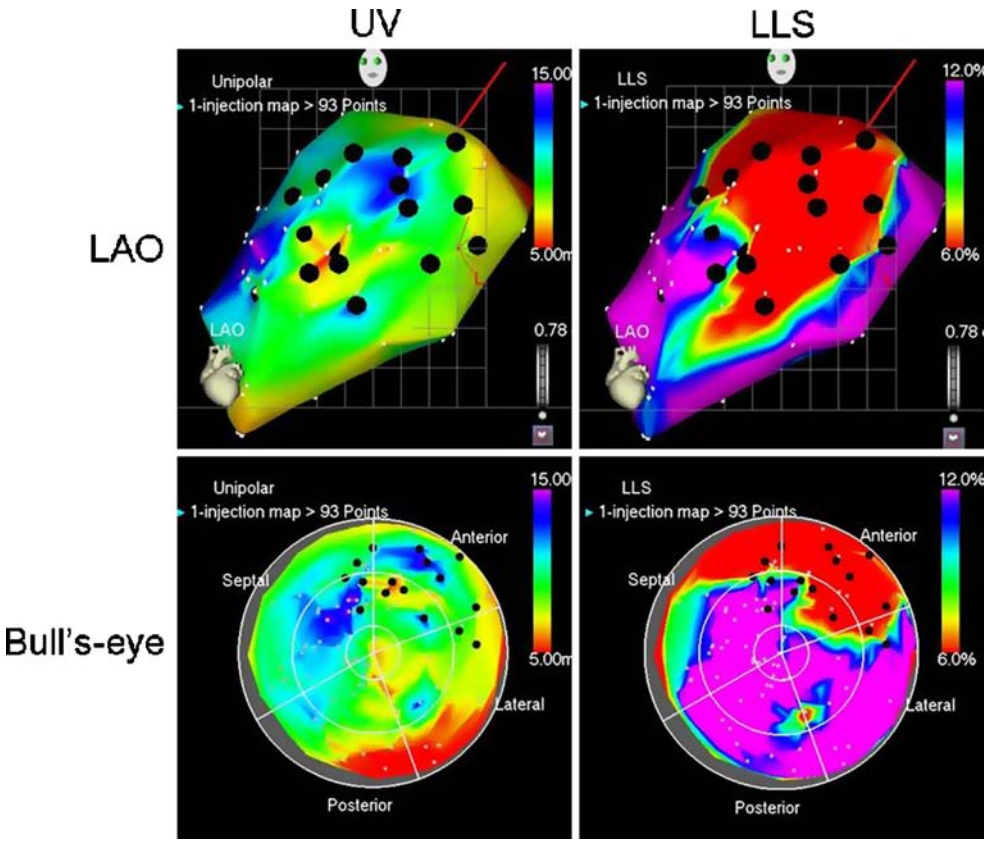

Fig. 3 Navigated injection for reversible myocardial ischemia. Left anterior oblique (LAO) and Bull's-eye representations of NOGA® XP injection maps in a subject with ischemic hibernating myocardium. Injections of cell therapy (*black circular markers*) were administered into the mid to basal anterior and antero-septal myocardium, where there was severe reduction of linear local shortening (LLS; *red area*), with intermediate reduction of unipolar voltage (UV; *yellow-green-blue areas*), implying contractile dysfunction but preserved viability. Images kindly provided by Dr. E.C. Perin, Texas Heart Institute, USA

recently demonstrated the effectiveness of NOGA®-guided, multisegmental delivery of allogeneic mesenchymal precursor cells in an ovine study of toxic cardiomyopathy ([60]; Psaltis et al. 2009b in submission). The same combination of cell type and delivery system is currently undergoing investigation in a clinical study of ischemic and NICM (www.clinicaltrials.gov NCT00721045).

Future Applications

Fertile areas of future research into cell-based therapy include the optimization of cell biology [27], the discovery of novel or second-generation cell types [4, 70], and the development of new delivery vectors [48] and strategies [36]. Key issues that remain unresolved relate to the optimal delivery route, timing, and dose of cell therapy in different cardiovascular diseases. The safety and efficacy of repeated versus single administration of treatment also warrant investigation [23], especially if beneficial outcomes remain transient due to poor levels of cell survival and engraftment.

There are currently over 50 NOGA® XP systems in clinical use worldwide, with numerous studies registered (www.clinicaltrials.gov). The phase II/III, multicenter C-Cure trial (NCT00810238) has recently commenced and is notable for investigating "guided BM-derived mesenchymal cardiopoietic cells" [4] in patients with ischemic cardiomyopathy. The placebo-controlled, REGEN-IHD study (NCT00747708) is also noteworthy as it is comparing three active treatment groups for ischemic cardiomyopathy: (1) subcutaneous injections of granulocyte-colony stimulating factor (G-CSF), (2) G-CSF with intracoronary infusion of BM cells, and (3) G-CSF with NOGA®-guided intramyocardial injection of BM cells.

With respect to technology, the NOGA® system continues to undergo various upgrades. The Windows XP platform has resulted in significant improvements compared to earlier generations, with easier user interface, better image visualization, and catheter response. The accuracy and precision of next generation NOGA® systems will be further enhanced by new software algorithms to compensate for the various sources of artifact (e.g., patient movement and variable cardiac cycle length). In addition, it is anticipated that anatomical and tissue characterization will be improved by integrating electromechanical map reconstructions with cardiac images obtained from other non-fluoroscopic modalities, such as MRI, computerized tomography, or real-time intracardiac echocardiography.

Modifications to catheter technology are also being trialed, including a multi-electrode catheter (QwikStar), which contains six sensors along its shaft in addition to the standard single tip electrode. Although this makes the catheter tip less flexible than the conventional NogaStar®, it enables data to be sampled simultaneously from multiple

sites, increasing point density and potentially shortening mapping time. Preliminary results indicate moderate-strong correlation with conventional, single-electrode mapping for segmental UV amplitude (Pearson's co-efficient 0.59–0.69 depending on point density), but not for LLS [17].

A new class of magnetically steerable catheters has also been developed for remote mapping and injection, by integrating NOGA® XP with the Stereotaxis magnetic navigation system (Niobe®, Stereotaxis, St. Louis, MO, USA). There are likely to be several advantages to this technology, including (1) further reduction of procedure time and radiation exposure, (2) the use of softer catheters with reduced risk of cardiac perforation, and (3) better catheter and needle accessibility to remote areas of the LV. Early results point to good efficiency for stereotactic injection, with deposition rates of approximately 95% and needle track penetration to greater than 50% of myocardial wall thickness [53].

Conclusion

Despite its imperfect diagnostic accuracy, the unique properties of electromechanical mapping make NOGA® an important tool for guiding intramyocardial interventions, including the delivery of cell therapy. The system's provision of 3D spatial orientation combined with real-time feedback (voltage potentials, endocardial shortening, electrogram, and catheter stability) assists the operator in targeting injection sites and assessing catheter stability and injection depth during cell transplantation. Ongoing modifications and the integration of adjuvant imaging modalities are expected to further enhance the technology's performance and strengthen its niche in the field of navigated cell delivery.

Acknowledgements The authors thank Dr. Emerson Perin and Mr. Fred Baimbridge (Texas Heart Institute, Houston, TX, USA) for kindly providing the image in Fig. 3. The authors have no financial conflicts to report. Dr. Psaltis is supported by a Postgraduate Medical Scholarship from the National Health and Medical Research Council of Australia (ID 390711) and the National Heart Foundation of Australia (PB 05A 2312) and a Dawes Scholarship from the Royal Adelaide Hospital.

References

1. Amado, L. C., Saliaris, A. P., Schuleri, K. H., St John, M., Xie, J. S., Cattaneo, S., et al. (2005). Cardiac repair with intramyocardial injection of allogeneic mesenchymal stem cells after myocardial infarction. *Proceedings of the National Academy of Sciences of the United States of America, 102*(32), 11474–11479.
2. Beeres, S. L., Bax, J. J., Dibbets-Schneider, P., Stokkel, M. P., Fibbe, W. E., van der Wall, E. E., et al. (2006). Sustained effect of autologous bone marrow mononuclear cell injection in patients with refractory angina pectoris and chronic myocardial ischemia: twelve-month follow-up results. *American Heart Journal, 152*(4), 684.e11–684.e16.
3. Beeres, S. L., Zeppenfeld, K., Bax, J. J., Dibbets-Schneider, P., Stokkel, M. P., Fibbe, W. E., et al. (2007). Electrophysiological and arrhythmogenic effects of intramyocardial bone marrow cell injection in patients with chronic ischemic heart disease. *Heart Rhythm, 4*(3), 257–265.
4. Behfar, A., Faustino, R. S., Arrell, D. K., Dzeja, P. P., Perez-Terzic, C., & Terzic, A. (2008). Guided stem cell cardiopoiesis: discovery and translation. *Journal of Molecular and Cellular Cardiology, 45*(4), 523–529.
5. Ben-Haim, S. A., Osadchy, D., Schuster, I., Gepstein, L., Hayam, G., & Josephson, M. E. (1996). Nonfluoroscopic, in vivo navigation and mapping technology. *Natural Medicines, 2*(12), 1393–1395.
6. Botker, H. E., Lassen, J. F., Hermansen, F., Wiggers, H., Sogaard, P., Kim, W. Y., et al. (2001). Electromechanical mapping for detection of myocardial viability in patients with ischemic cardiomyopathy. *Circulation, 103*(12), 1631–1637.
7. Chazaud, B., Hittinger, L., Sonnet, C., Champagne, S., Le Corvoisier, P., Benhaiem-Sigaux, N., et al. (2003). Endoventricular porcine autologous myoblast transplantation can be successfully achieved with minor mechanical cell damage. *Cardiovascular Research, 58*(2), 444–450.
8. Cheng, Y., Sherman, W., Yi, G., Conditt, G., Sheehy, A., Martens, T., et al. (2009). Real time 3D echo guided intramyocardial delivery of mesenchymal precursor cells in a chronic myocardial infarct ovine model using a novel catheter. *Journal of the American College of Cardiology, 53*(10 Suppl A), A41.
9. Corti, R., Badimon, J., Mizsei, G., Macaluso, F., Lee, M., Licato, P., et al. (2005). Real time magnetic resonance guided endomyocardial local delivery. *Heart, 91*(3), 348–353.
10. de Leeuw, N., Ruiter, D. J., Balk, A. H., de Jonge, N., Melchers, W. J., & Galama, J. M. (2001). Histopathologic findings in explanted heart tissue from patients with end-stage idiopathic dilated cardiomyopathy. *Transplant International, 14*(5), 299–306.
11. de Silva, R., Gutierrez, L. F., Raval, A. N., McVeigh, E. R., Ozturk, C., & Lederman, R. J. (2006). X-ray fused with magnetic resonance imaging (XFM) to target endomyocardial injections: validation in a swine model of myocardial infarction. *Circulation, 114*(22), 2342–2350.
12. Dib, N., Dinsmore, J., Lababidi, Z., White, B., Moravec, S., Campbell, A., et al. (2009). One-year follow-up of feasibility and safety of the first U.S., randomized, controlled study using 3-dimensional guided catheter-based delivery of autologous skeletal myoblasts for ischemic cardiomyopathy (CAuSMIC study). *JACC Cardiovascular Interventions, 2*(1), 9–16.
13. Dick, A. J., Guttman, M. A., Raman, V. K., Peters, D. C., Pessanha, B. S., Hill, J. M., et al. (2003). Magnetic resonance fluoroscopy allows targeted delivery of mesenchymal stem cells to infarct borders in Swine. *Circulation, 108*(23), 2899–2904.
14. Dohmann, H. F., Perin, E. C., Takiya, C. M., Silva, G. V., Silva, S. A., Sousa, A. L., et al. (2005). Transendocardial autologous bone marrow mononuclear cell injection in ischemic heart failure: postmortem anatomicopathologic and immunohistochemical findings. *Circulation, 112*(4), 521–526.
15. Erbs, S., Linke, A., Adams, V., Lenk, K., Thiele, H., Diederich, K. W., et al. (2005). Transplantation of blood-derived progenitor cells after recanalization of chronic coronary artery occlusion: first randomized and placebo-controlled study. *Circulation Research, 97*(8), 756–762.
16. Fernandes, M. R., Silva, G., Cardoso, C. O., Zheng, Y., Baimbridge, F., Cabreira, M. G., et al. (2009). The impact of timing on the safety of transendocardial delivery of mesenchymal precursor stem cells following acute myocardial infarction. *Journal of the American College of Cardiology, 53*(10 Suppl A), A311.

17. Fernandes, M. R., Silva, G. V., Zheng, Y., Oliveira, E. M., Cardoso, C. O., Canales, J., et al. (2008). Validation of QwikStar catheter for left ventricular electromechanical mapping with NOGA XP system. *Texas Heart Institute Journal, 35*(3), 240–244.
18. Fischer-Rasokat, U., Assmus, B., Seeger, F. H., Honold, J., Leistner, D., Fichtlscherer, S., et al. (2009). A pilot trial to assess potential effects of selective intracoronary bone marrow-derived progenitor cell infusion in patients with non-ischemic dilated cardiomyopathy: Final 1-year results of the TOPCARE-DCM trial. *Circulation Heart Failure, 2*, 417–423.
19. Freyman, T., Polin, G., Osman, H., Crary, J., Lu, M., Cheng, L., et al. (2006). A quantitative, randomized study evaluating three methods of mesenchymal stem cell delivery following myocardial infarction. *European Heart Journal, 27*(9), 1114–1122.
20. Fuchs, S., Hendel, R. C., Baim, D. S., Moses, J. W., Pierre, A., Laham, R. J., et al. (2001). Comparison of endocardial electromechanical mapping with radionuclide perfusion imaging to assess myocardial viability and severity of myocardial ischemia in angina pectoris. *American Journal of Cardiology, 87*(7), 874–880.
21. Fuchs, S., Kornowski, R., Shiran, A., Pierre, A., Ellahham, S., & Leon, M. B. (1999). Electromechanical characterization of myocardial hibernation in a pig model. *Coronary Artery Disease, 10*(3), 195–198.
22. Fuchs, S., Kornowski, R., Weisz, G., Satler, L. F., Smits, P. C., Okubagzi, P., et al. (2006). Safety and feasibility of transendocardial autologous bone marrow cell transplantation in patients with advanced heart disease. *American Journal of Cardiology, 97*(6), 823–829.
23. Gavira, J. J., Nasarre, E., Abizanda, G., Perez-Ilzarbe, M., de Martino-Rodriguez, A., Garcia de Jalon, J. A., et al. (2009). Repeated implantation of skeletal myoblast in a swine model of chronic myocardial infarction. *European Heart Journal*, (in press).
24. Gavira, J. J., Perez-Ilzarbe, M., Abizanda, G., Garcia-Rodriguez, A., Orbe, J., Paramo, J. A., et al. (2006). A comparison between percutaneous and surgical transplantation of autologous skeletal myoblasts in a swine model of chronic myocardial infarction. *Cardiovascular Research, 71*(4), 744–753.
25. Gepstein, L., Hayam, G., & Ben-Haim, S. A. (1997a). A novel method for nonfluoroscopic catheter-based electroanatomical mapping of the heart. In vitro and in vivo accuracy results. *Circulation, 95*(6), 1611–1622.
26. Gepstein, L., Hayam, G., Shpun, S., & Ben-Haim, S. A. (1997b). Hemodynamic evaluation of the heart with a nonfluoroscopic electromechanical mapping technique. *Circulation, 96*(10), 3672–3680.
27. Gnecchi, M., He, H., Liang, O. D., Melo, L. G., Morello, F., Mu, H., et al. (2005). Paracrine action accounts for marked protection of ischemic heart by Akt-modified mesenchymal stem cells. *Natural Medicines, 11*(4), 367–368.
28. Gnecchi, M., Zhang, Z., Ni, A., & Dzau, V. J. (2008). Paracrine mechanisms in adult stem cell signaling and therapy. *Circulation Research, 103*(11), 1204–1219.
29. Graf, S., Gyongyosi, M., Khorsand, A., Nekolla, S. G., Pirich, C., Kletter, K., et al. (2004). Electromechanical properties of perfusion/metabolism mismatch: comparison of nonfluoroscopic electroanatomic mapping with 18F-FDG PET. *Journal of Nuclear Medicine, 45*(10), 1611–1618.
30. Grossman, P. M., Han, Z., Palasis, M., Barry, J. J., & Lederman, R. J. (2002). Incomplete retention after direct myocardial injection. *Catheterization and Cardiovascular Interventions, 55*(3), 392–397.
31. Gyongyosi, M., Lang, I., Dettke, M., Beran, G., Graf, S., Sochor, H., et al. (2009). Combined delivery approach of bone marrow mononuclear stem cells early and late after myocardial infarction: the MYSTAR prospective, randomized study. *Nature Clinical Practice Cardiovascular Medicine, 6*(1), 70–81.
32. Heng, B. C., Hsu, S. H., Cowan, C. M., Liu, A., Tai, J., Chan, Y., et al. (2009). Trans-catheter injection induced changes in human bone marrow-derived mesenchymal stem cells. *Cell Transplant* (in press).
33. Hou, D., Youssef, E. A., Brinton, T. J., Zhang, P., Rogers, P., Price, E. T., et al. (2005). Radiolabeled cell distribution after intramyocardial, intracoronary, and interstitial retrograde coronary venous delivery: implications for current clinical trials. *Circulation, 112*(9 Suppl), I150–I156.
34. Hsia, H. H., & Marchlinski, F. E. (2002). Characterization of the electroanatomic substrate for monomorphic ventricular tachycardia in patients with nonischemic cardiomyopathy. *Pacing and Clinical Electrophysiology, 25*(7), 1114–1127.
35. Ince, H., Petzsch, M., Rehders, T. C., Chatterjee, T., & Nienaber, C. A. (2004). Transcatheter transplantation of autologous skeletal myoblasts in postinfarction patients with severe left ventricular dysfunction. *Journal of Endovascular Therapy, 11*(6), 695–704.
36. Kaye, D. M., Preovolos, A., Marshall, T., Byrne, M., Hoshijima, M., Hajjar, R., et al. (2007). Percutaneous cardiac recirculation-mediated gene transfer of an inhibitory phospholamban peptide reverses advanced heart failure in large animals. *Journal of the American College of Cardiology, 50*(3), 253–260.
37. Keck, A., Hertting, K., Schwartz, Y., Kitzing, R., Weber, M., Leisner, B., et al. (2002). Electromechanical mapping for determination of myocardial contractility and viability. A comparison with echocardiography, myocardial single-photon emission computed tomography, and positron emission tomography. *Journal of the American College of Cardiology, 40*(6), 1067–1074.
38. Kornowski, R., Fuchs, S., Shiran, A., Summers, N., Pietrusewicz, M., Ellahham, S., et al. (2001). Catheter-based electromechanical mapping to assess regional myocardial function: a comparative analysis with transthoracic echocardiography. *Catheterization and Cardiovascular Interventions, 52*(3), 342–347.
39. Kornowski, R., Hong, M. K., Gepstein, L., Goldstein, S., Ellahham, S., Ben-Haim, S. A., et al. (1998a). Preliminary animal and clinical experiences using an electromechanical endocardial mapping procedure to distinguish infarcted from healthy myocardium. *Circulation, 98*(11), 1116–1124.
40. Kornowski, R., Hong, M. K., & Leon, M. B. (1998b). Comparison between left ventricular electromechanical mapping and radionuclide perfusion imaging for detection of myocardial viability. *Circulation, 98*(18), 1837–1841.
41. Kornowski, R., Leon, M. B., Fuchs, S., Vodovotz, Y., Flynn, M. A., Gordon, D. A., et al. (2000). Electromagnetic guidance for catheter-based transendocardial injection: a platform for intramyocardial angiogenesis therapy. Results in normal and ischemic porcine models. *Journal of the American College of Cardiology, 35*(4), 1031–1039.
42. Krause, K., Jaquet, K., Schneider, C., Haupt, S., Lioznov, M. V., Otte, K. M., et al. (2009). Percutaneous intramyocardial stem cell injection in patients with acute myocardial infarction: first-in-man study. *Heart, 95*(14), 1145–1152.
43. Lau, G. T., Yoneyama, R., Kawase, Y., Ly, H. Q., Hoshino, K., Pomerantseva, I., et al. (2009). Accuracy of non-fluoroscopic cather based electromechanically-guided (NOGA) mononuclear cell endocardial injection in a swine myocardial infarction model assessed by MRI. *Heart, Lung and Circulation, 18*(Suppl 3), S73.
44. Leon, M. B., Kornowski, R., Downey, W. E., Weisz, G., Baim, D. S., Bonow, R. O., et al. (2005). A blinded, randomized, placebo-controlled trial of percutaneous laser myocardial revascularization to improve angina symptoms in patients with severe coronary disease. *Journal of the American College of Cardiology, 46*(10), 1812–1819.
45. Leri, A., Kajstura, J., & Anversa, P. (2005). Cardiac stem cells and mechanisms of myocardial regeneration. *Physiological Reviews, 85*(4), 1373–1416.

46. Losordo, D. W., Schatz, R. A., White, C. J., Udelson, J. E., Veereshwarayya, V., Durgin, M., et al. (2007). Intramyocardial transplantation of autologous CD34+ stem cells for intractable angina: a phase I/IIa double-blind, randomized controlled trial. *Circulation, 115*(25), 3165–3172.
47. Martens, T. P., Godier, A. F., Parks, J. J., Wan, L. Q., Koeckert, M. S., Eng, G. M., et al. (2009). Percutaneous cell delivery into the heart using hydrogels polymerizing in situ. *Cell Transplantation, 18*(3), 297–304.
48. Menasche, P., Alfieri, O., Janssens, S., McKenna, W., Reichenspurner, H., Trinquart, L., et al. (2008). The myoblast autologous grafting in ischemic cardiomyopathy (MAGIC) trial: first randomized placebo-controlled study of myoblast transplantation. *Circulation, 117*(9), 1189–1200.
49. Opie, S. R., & Dib, N. (2006). Surgical and catheter delivery of autologous myoblasts in patients with congestive heart failure. *Nature Clinical Practice Cardiovascular Medicine, 3*(Suppl 1), S42–S45.
50. Perin, E. C., Dohmann, H. F., Borojevic, R., Silva, S. A., Sousa, A. L., Mesquita, C. T., et al. (2003). Transendocardial, autologous bone marrow cell transplantation for severe, chronic ischemic heart failure. *Circulation, 107*(18), 2294–2302.
51. Perin, E. C., Dohmann, H. F., Borojevic, R., Silva, S. A., Sousa, A. L., Silva, G. V., et al. (2004). Improved exercise capacity and ischemia 6 and 12 months after transendocardial injection of autologous bone marrow mononuclear cells for ischemic cardiomyopathy. *Circulation, 110*(11 Suppl 1), II213–II218.
52. Perin, E. C., Silva, G. V., Assad, J. A., Vela, D., Buja, L. M., Sousa, A. L., et al. (2008). Comparison of intracoronary and transendocardial delivery of allogeneic mesenchymal cells in a canine model of acute myocardial infarction. *Journal of Molecular and Cellular Cardiology, 44*(3), 486–495.
53. Perin, E. C., Silva, G. V., Fernandes, M. R., Munger, T., Pandey, A., Sehra, R., et al. (2007). First experience with remote left ventricular mapping and transendocardial cell injection with a novel integrated magnetic navigation-guided electromechanical mapping system. *Eurointervention, 3*(1), 142–148.
54. Perin, E. C., Silva, G. V., Sarmento-Leite, R., Sousa, A. L., Howell, M., Muthupillai, R., et al. (2002). Assessing myocardial viability and infarct transmurality with left ventricular electromechanical mapping in patients with stable coronary artery disease: validation by delayed-enhancement magnetic resonance imaging. *Circulation, 106*(8), 957–961.
55. Poh, K. K., Sperry, E., Young, R. G., Freyman, T., Barringhaus, K. G., & Thompson, C. A. (2007). Repeated direct endomyocardial transplantation of allogeneic mesenchymal stem cells: safety of a high dose, "off-the-shelf", cellular cardiomyoplasty strategy. *International Journal of Cardiology, 117*(3), 360–364.
56. Pompilio, G., Steinhoff, G., Liebold, A., Pesce, M., Alamanni, F., Capogrossi, M. C., et al. (2008). Direct minimally invasive intramyocardial injection of bone marrow-derived AC133+ stem cells in patients with refractory ischemia: preliminary results. *Thoracic and Cardiovascular Surgeon, 56*(2), 71–76.
57. Poppas, A., Sheehan, F. H., Reisman, M., Harms, V., & Kornowski, R. (2004). Validation of viability assessment by electromechanical mapping by three-dimensional reconstruction with dobutamine stress echocardiography in patients with coronary artery disease. *American Journal of Cardiology, 93*(9), 1097–1101.
58. Psaltis, P. J., Carbone, A., Nelson, A., Lau, D. H., Manavis, J., Finnie, J., et al. (2008a). An ovine model of toxic, nonischemic cardiomyopathy—assessment by cardiac magnetic resonance imaging. *Journal of Cardiac Failure, 14*(9), 785–795.
59. Psaltis, P. J., Gronthos, S., Worthley, S. G., & Zannettino, A. C. W. (2008b). Cellular therapy for cardiovascular disease part 2—delivery of cells and clinical experience. *Clinical Medicine: Cardiology, 2*, 139–151.
60. Psaltis, P. J., Nelson, A. J., Carbone, A., Lau, D. H., Jantzen, T., Williams, K., et al. (2009). Cardiac repair with intramyocardial injection of allogeneic mesenchymal precursor cells for experimental nonischaemic cardiomyopathy. *Heart, Lung and Circulation, 18*(Suppl 3), S74.
61. Psaltis, P. J., & Worthley, S. G. (2009). Endoventricular electromechanical mapping—the diagnostic and therapeutic utility of the NOGA® XP Cardiac Navigation System. *Journal of Cardiovascular Translational Research, 2*(1), 48–62.
62. Psaltis, P. J., Zannettino, A. C., Worthley, S. G., & Gronthos, S. (2008c). Concise review: mesenchymal stromal cells: potential for cardiovascular repair. *Stem Cells, 26*(9), 2201–2210.
63. Rezaee, M., Yeung, A. C., Altman, P., Lubbe, D., Takeshi, S., Schwartz, R. S., et al. (2001). Evaluation of the percutaneous intramyocardial injection for local myocardial treatment. *Catheterization and Cardiovascular Interventions, 53*(2), 271–276.
64. Schachinger, V., Erbs, S., Elsasser, A., Haberbosch, W., Hambrecht, R., Holschermann, H., et al. (2006). Intracoronary bone marrow-derived progenitor cells in acute myocardial infarction. *New England Journal of Medicine, 355*(12), 1210–1221.
65. Siminiak, T., Fiszer, D., Jerzykowska, O., Grygielska, B., Rozwadowska, N., Kalmucki, P., et al. (2005). Percutaneous trans-coronary-venous transplantation of autologous skeletal myoblasts in the treatment of post-infarction myocardial contractility impairment: the POZNAN trial. *European Heart Journal, 26*(12), 1188–1195.
66. Smeets, J. L., Ben-Haim, S. A., Rodriguez, L. M., Timmermans, C., & Wellens, H. J. (1998). New method for nonfluoroscopic endocardial mapping in humans: accuracy assessment and first clinical results. *Circulation, 97*(24), 2426–2432.
67. Smits, P. C., van Geuns, R. J., Poldermans, D., Bountioukos, M., Onderwater, E. E., Lee, C. H., et al. (2003). Catheter-based intramyocardial injection of autologous skeletal myoblasts as a primary treatment of ischemic heart failure: clinical experience with six-month follow-up. *Journal of the American College of Cardiology, 42*(12), 2063–2069.
68. Smits, P. C., van Langenhove, G., Schaar, M., Reijs, A., Bakker, W. H., van der Giessen, W. J., et al. (2002). Efficacy of percutaneous intramyocardial injections using a nonfluoroscopic 3-D mapping based catheter system. *Cardiovascular Drugs and Therapy, 16*(6), 527–533.
69. Steendijk, P., Smits, P. C., Valgimigli, M., van der Giessen, W. J., Onderwater, E. E., & Serruys, P. W. (2006). Intramyocardial injection of skeletal myoblasts: long-term follow-up with pressure-volume loops. *Nature Clinical Practice Cardiovascular Medicine, 3*(Suppl 1), S94–S100.
70. Takahashi, K., & Yamanaka, S. (2006). Induction of pluripotent stem cells from mouse embryonic and adult fibroblast cultures by defined factors. *Cell, 126*(4), 663–676.
71. Theiss, H. D., David, R., Engelmann, M. G., Barth, A., Schotten, K., Naebauer, M., et al. (2007). Circulation of CD34+ progenitor cell populations in patients with idiopathic dilated and ischaemic cardiomyopathy (DCM and ICM). *European Heart Journal, 28*(10), 1258–1264.
72. Tse, H. F., Thambar, S., Kwong, Y. L., Rowlings, P., Bellamy, G., McCrohon, J., et al. (2007). Prospective randomized trial of direct endomyocardial implantation of bone marrow cells for treatment of severe coronary artery diseases (PROTECT-CAD trial). *European Heart Journal, 28*(24), 2998–3005.
73. Vale, P. R., Losordo, D. W., Milliken, C. E., Maysky, M., Esakof, D. D., Symes, J. F., et al. (2000). Left ventricular electromechanical mapping to assess efficacy of phVEGF(165) gene transfer for therapeutic angiogenesis in chronic myocardial ischemia. *Circulation, 102*(9), 965–974.

74. Vale, P. R., Losordo, D. W., Tkebuchava, T., Chen, D., Milliken, C. E., & Isner, J. M. (1999). Catheter-based myocardial gene transfer utilizing nonfluoroscopic electromechanical left ventricular mapping. *Journal of the American College of Cardiology, 34* (1), 246–254.
75. van Ramshorst, J., Bax, J. J., Beeres, S. L., Dibbets-Schneider, P., Roes, S. D., Stokkel, M. P., et al. (2009). Intramyocardial bone marrow cell injection for chronic myocardial ischemia: a randomized controlled trial. *Journal of the American Medical Association, 301*(19), 1997–2004.
76. Vulliet, P. R., Greeley, M., Halloran, S. M., MacDonald, K. A., & Kittleson, M. D. (2004). Intra-coronary arterial injection of mesenchymal stromal cells and microinfarction in dogs. *Lancet, 363*(9411), 783–784.
77. Wiggers, H., Botker, H. E., Sogaard, P., Kaltoft, A., Hermansen, F., Kim, W. Y., et al. (2003). Electromechanical mapping versus positron emission tomography and single photon emission computed tomography for the detection of myocardial viability in patients with ischemic cardiomyopathy. *Journal of the American College of Cardiology, 41*(5), 843–848.
78. Wolf, T., Gepstein, L., Dror, U., Hayam, G., Shofti, R., Zaretzky, A., et al. (2001). Detailed endocardial mapping accurately predicts the transmural extent of myocardial infarction. *Journal of the American College of Cardiology, 37*(6), 1590–1597.